Journal of Zhejiang University-SCIENCE A (Applied Physics & Engineering)
ISSN 1673-565X (Print); ISSN 1862-1775 (Online)
www.jzus.zju.edu.cn; www.springerlink.com
E-mail: jzus@zju.edu.cn

Co-benefit of hazardous trace elements capture in dust removal devices of ultra-low emission coal-fired power plants*#

Cheng-hang ZHENG, Li WANG, Yong-xin ZHANG,
Wei-guo WENG, Hai-tao ZHAO, Jin-song ZHOU, Xiang GAO†‡

State Key Laboratory of Clean Energy Utilization, State Environmental Protection Center for Coal-fired Air Pollution Control, Zhejiang University, Hangzhou 310027, China

†E-mail: xgao1@zju.edu.cn

Received Apr. 26, 2017; Revision accepted Sept. 9, 2017; Crosschecked Dec. 15, 2017

Abstract: The co-benefit of hazardous trace elements such as mercury (Hg), arsenic (As), and selenium (Se) capture in dust removal devices of ultra-low emission coal-fired power plants was investigated. Feed fuel and ash samples collected from 15 different coal-fired power units equipped with ultra-low emission systems were characterized to determine the concentrations and distribution characteristics of trace elements. It was found that the low-low temperature electrostatic precipitator (LLT-ESP) and the electrostatic fabric filter (EFF) had greater abatement capacity for Hg than normal cold-side ESP (CS-ESP). Only 0.8%–36.1% of Hg escaped from LLT-ESP and EFF, whereas 42.1%–90.6% of Hg escaped from CS-ESP. With the employment of EFF and ESP (inlet temperature<125 °C), 72.3%–99.1% of As and 70.7%–100% of Se could be captured before the wet flue gas desulfurization (WFGD) system. The significance level of the effects on the abatement capacity for Hg, As, and Se in ESP were analyzed by the Pearson correlation analysis and grey relational analysis. The results indicated that the low inlet temperature of LLT-ESP had significant promotional effect on the simultaneous removal of Hg, As, and Se. The smaller particle size of fly ash can be conducive to the adsorption of hazardous trace elements. The inhibitory effect of sulfur content in coal was significant for the enrichment of Hg and Se in fly ash.

Key words: Trace elements; Abatement capacity; Low-low temperature electrostatic precipitator (LLT-ESP); Electrostatic fabric filter (EFF); Influencing factors

https://doi.org/10.1631/jzus.A1700229 **CLC number:** TH161.12

1 Introduction

Coal is the dominant fuel for power generation in China. During coal combustion, hazardous trace elements such as mercury (Hg), arsenic (As), and selenium (Se) are first volatilized and subsequently partition into bottom ash, fly ash, and flue gas. The atmospheric emissions of Hg, As, and Se can cause a significant negative impact on the environment and public health (Tian et al., 2014). This has received worldwide attention. The US Environmental Protection Agency (EPA) announced Mercury and Air Toxics Standards (MATS) for Power Plants on Dec. 21, 2011 (Futsaeter and Wilson, 2013). The Chinese government promulgated the latest Emission Standard of Air Pollutants for Thermal Power Plants, which restricted the emission limit of Hg for the first time (MEP, 2011). The formulation of relevant emission limits for Se and As is in progress.

---

‡ Corresponding author

[*] Project supported by the National Key Research and Development Plan (No. 2016YFC0203706), the National Natural Science Foundation of China (Nos. U1609212 and 51621005), and the Environmental Welfare Project of the Ministry of Environmental Projection of China (No. 201509012)

[#] Electronic supplementary materials: The online version of this article (https://doi.org/10.1631/jzus.A1700229) contains supplementary materials, which are available to authorized users

ORCID: Xiang GAO, https://orcid.org/0000-0002-1732-2132; Cheng-hang ZHENG, https://orcid.org/0000-0003-0410- 2007

The utilization of installed air pollution control devices has been acknowledged as the most promising way to control the emission of hazardous trace elements. Dust removal devices such as the electrostatic precipitator (ESP) and the fabric filter (FF) have a potential abatement capacity for trace elements. ESP and FF can effectively remove the particulate bound Hg, As, and Se by capturing the fly ash. The removal efficiency of Hg by ESP/EFF (electrostatic fabric filter) varied from 5% to 91% (Lopez-Anton et al., 2006; Deng et al., 2014; Zhou et al., 2015; Zhang et al., 2016). This heavily depended on the ratio of Hg^p in Hg^T and the oxidation efficiency of Hg^0 (Gao et al., 2013). Physical adsorption played an important role for Se (Chen et al., 2001) and the distribution of Se in fly ash varied from 49%–98% (Tian et al., 2010). The simultaneous effect of chemical and physical adsorption determined the enrichment of As in fly ash. The removal efficiency of As in ESP/EFF ranged from 35% to 99% (Cheng et al., 2009; Tian et al., 2010).

Ultra-low emission technologies have been widely applied in coal fired power plants in China to meet strict emission standards. The technologies include the high efficiency selective catalytic reduction system (SCR), the low-low temperature ESP (LLT-ESP)/EFF, the wet flue gas desulfurization (WFGD) and wet electrostatic precipitator (WESP) systems, where the particulate matters (PM), SO_2, and NO_x emissions can be limited to 5, 35, and 50 mg/m^3, respectively. LLT-ESP and EFF are the typical ultra-low emission dust removal devices. LLT-ESP is employed to lower the ESP inlet gas temperature below the acid dew point (typically below 95 °C) using a low-temperature economizer or hot media gas–gas heat exchanger (Fu and Ma, 2014). The basic principle of the EFF is that 70%–90% of the dust is collected by ESP and the rest of the pre-charged particulates will be removed by the fabric filter. It can be ensured that the emission concentration of PM is less than 20 mg/m^3 before WFGD. The development of this kind of dust removal device may have an enormous effect on the control of trace elements. However, little research has focused on the capturing of trace elements at lower temperatures, i.e. <95 °C in LLT-ESP.

Various factors such as coal type, flue gas components, characteristics of the fly ash and the operational parameters of dust removal devices can affect the removal efficiency of Hg, As, and Se (Kellie et al., 2005; Hower et al., 2010; Wilcox et al., 2012; Burmistrz et al., 2016; Zhang et al., 2016). Better understanding of influencing factors on the abatement capacity for trace elements can be conducive to furthering plans for trace element control strategy.

In this study, the concentrations and distributions of Hg, As, and Se in coal, bottom ash, and fly ash were investigated in 15 ultra-low emission coal-fired power plants equipped with LLT-ESP, CS-ESP, and EFF. The abatement capacity for trace elements in different dust removal devices was examined. The degree of correlation between influencing factors and enrichment of Hg, As, and Se in fly ash was analyzed by Pearson coefficients and the significance level of different factors was obtained through grey relational analysis.

2 Experimental

2.1 Description of coal fired power units

Fifteen coal fired power plants equipped with LLT-ESP, normal CS-ESP, and EFF were selected. The details of the tested coal fired power units are listed in Table 1. Pulverized coal (PC) boilers were utilized in units #1–#12 with installed capacity ranging from 220 MW to 1000 MW. Circulating fluidized bed (CFB) boilers were used in units #13–#15. Waste sludge was blended in the coal in units #14 and #15. LLT-ESP systems were employed in units #1–#4. Normal CS-ESP systems were installed in units #5–#12. EFF systems were installed in units #13–#15. All tested units were equipped with SCR systems and WFGD systems to control NO_x and SO_2. Selective non-catalytic reduction (SNCR) combined with SCR was employed in units #14 and #15. The WESP system was installed downstream of WFGD systems to further remove ultra-fine particles, carryovers, and other pollutants.

The proximate analysis, total sulfur and chorine analysis, concentrations of trace elements, and the oxides content of feed fuels are shown in Table 2. The coal properties varied: the sulfur content in coal ranged from 0.45%–3.5%, ash content ranged from 11.99%–31.48%, and volatile matter varied from 10.7% to 33.07%. The Hg content in feed fuels ranged from 0.02 mg/kg to 0.15 mg/kg with a mean value of

0.09 mg/kg. The concentrations of As and Se were in the range of 0.37 mg/kg–13.45 mg/kg (mean value: 5.47 mg/kg) and 0.87 mg/kg to 5.09 mg/kg (mean value: 2.77 mg/kg), respectively.

2.2 Sample collection and analysis

The coal samples were obtained from samples located at the coal feeder of the boilers. Bottom ash samples were collected from the slag discharge system of the boilers and fly ash was collected from the hoppers of the ESP or EFF. The sampling campaigns were carried out under continuous operating conditions with the boiler loads deviations maintained within ±5%.

The coal and bottom ash samples were manually ground to obtain a representative subsample of particle size <250 μm for further chemical tests. The proximate analysis of coal was determined based on GB/T212-2008 (GAQSIQ, 2008). Total sulfur content in coal (S) and chlorine content in coal (Cl) were measured based on GB/T 214-2007 (GAQSIQ, 2007) and GB/T 3558-2014 (GAQSIQ, 2014), respectively. The fly ash and bottom ash samples were first digested by a HF-HNO_3 solution in a microwave oven and the recovered solution samples were analyzed for As and Se using inductively coupled plasma mass spectrometry (ICP-MS) (XSENIES II, Thermo Fisher Scientific, America). The content of Hg in samples

Table 1 Details of coal fired power units

Unit	Installed capacity (MW)	Boiler type	Coal type	Type of DRD^a	T (°C)^b
#1	1000	PC	Bit^c	LLT^f	90
#2	1000	PC	bit	LLT	87
#3	660	PC	bit	LLT	92
#4	660	PC	bit	LLT	94
#5	660	PC	bit	CS^g	118
#6	300	PC	Bit	CS	115
#7	660	PC	bit	CS	125
#8	220	PC	bit	CS	120
#9	330	PC	bit	CS	132
#10	330	PC	bit+lig^d	CS	128
#11	330	PC	bit	CS	145
#12	300	PC	bit	CS	140
#13	220	CFB	bit	EFF	118
#14	50	CFB	bit+S^e	EFF	120
#15	50	CFB	bit+S	EFF	122

^{a} Dust removal devices; ^{b} Inlet temperature of ESP/EFF (°C); ^{c} Bituminous coal; ^{d} Lignite; ^{e} Sludge; ^{f} Low-low temperature ESP; ^{g} Cold-side ESP

Table 2 Proximate analysis, total sulfur and chorine analysis, and the concentrations of trace metals in feed fuel

Unit	Ultimate analysis (%, in weight)				S	Cl	Trace elements (mg/kg)			Oxides (%)			
	Mad	Aad	Vad	FCad	(%)	(mg/kg)	Hg	As	Se	SiO_2	Al_2O_3	CaO	Fe_2O_3
#1	5.30	11.99	30.90	51.81	0.84	145	0.07	5.29	1.32	6.44	3.38	1.20	0.57
#2	7.60	12.89	28.08	51.43	0.48	205	0.02	3.80	0.87	4.51	2.41	1.08	0.53
#3	4.11	18.11	28.96	48.82	0.80	285	0.12	6.94	3.12	6.25	5.69	0.55	0.54
#4	12.60	16.89	28.06	49.15	0.45	465	0.06	3.96	2.15	5.05	3.42	1.13	0.40
#5	6.27	13.28	30.23	50.24	0.58	151	0.03	2.91	2.65	8.17	7.04	1.30	0.53
#6	2.09	18.94	36.91	44.16	0.61	290	0.08	7.07	4.77	6.02	5.59	0.71	0.40
#7	2.78	22.26	28.55	46.42	0.70	103	0.14	5.34	3.36	6.43	6.52	0.83	0.45
#8	1.49	30.36	10.70	58.09	1.22	500	0.11	8.95	4.27	9.14	6.24	0.37	0.54
#9	2.47	18.71	29.37	49.45	0.56	110	0.12	0.37	1.08	9.45	8.06	0.66	0.56
#10	1.49	31.48	26.58	40.45	1.70	127	0.11	1.20	1.78	6.21	7.44	1.08	0.59
#11	3.38	22.23	28.21	46.18	2.10	174	0.15	3.17	2.74	7.78	7.33	0.89	0.35
#12	2.97	18.98	23.43	54.62	3.50	67	0.08	4.42	1.39	8.91	5.13	0.83	0.91
#13	1.76	29.72	12.65	55.88	1.20	723	0.07	5.81	3.41	8.95	5.82	0.62	0.69
#14	5.28	31.05	33.07	30.60	1.35	468	0.09	9.40	5.09	4.12	4.57	4.27	2.93
#15	4.32	30.01	32.80	32.87	1.01	670	0.07	13.45	3.56	7.55	5.15	3.56	4.20

was directly measured by a Lumex RA–915M mercury analyzer with PYRO–915+ pyrolysis equipment. X-ray fluorescence (ADVANT'X 4200, ThermoFisher Scientific, USA) was used to determine the content of oxides (CaO, Fe_2O_3, and SO_x) in fly ash and bottom ash. Photo-micrographs were obtained using a scanning electron microscope (SEM) (SU-70 Hitachi, Japan). The median particle size of the fly ash was determined by a Malvern Particle Size Analyzer (Mastersizer 2000, USA). All samples were tested in triplicate, and the measurement errors were maintained within ±5%.

2.3 Mathematical analysis method

Grey relational analysis was employed in order to quantitatively analyze the significance level of influencing factors on the enrichment of trace elements in fly ash. Grey relational analysis is a widely acknowledged method for multi-criteria decisions (Kuo et al., 2008). According to grey relational analysis, if two factors have a higher degree of synchronous change in the process of system development, it is considered that the correlation between the two factors is larger; conversely, the two factors have smaller correlation. The key of the analysis is to calculate the grey relational grade r_i (the subscript i denotes the factors). If the grey relational grade value is closer to unity, the correlation is stronger.

The detailed data processing of grey relational analysis in this study is as follows: Firstly, the original sequence was normalized by letting the values of the original sequence be divided by the average value of the sequence (if the correlation between factors was negative, the reciprocal of the original sequence should be a substitute for the original sequence). Secondly, the deviation sequences of the reference sequence and the comparability sequences ($\Delta_i(k)$) were calculated, and the maximum and minimum values of the deviation were obtained.

$$\Delta_i(k) = | X_{\mathrm{REF}}(k) - X_i(k) |, \tag{1}$$

$$\Delta_{\max} = \max_i(\max_k(\Delta_i(k))), \tag{2}$$

$$\Delta_{\min} = \min_i(\min_k(\Delta_i(k))), \quad k = 1, 2, 3, \cdots, \tag{3}$$

where k denotes the number of tested units, $X_{\mathrm{REF}}(k)$ denotes the value of relative enrichment factor (REF), and $X_i(k)$ denotes the influencing factors.

The grey relation coefficient $\xi_i(k)$ can be calculated by

$$\xi_i(k) = \frac{\Delta_{\min} + \rho\Delta_{\max}}{\Delta_i(k) + \rho\Delta_{\max}}, \quad k = 1, 2, 3, \cdots, \tag{4}$$

where ρ is the identification coefficient: $\rho \in [0, 1]$. The smaller the value of ρ is, the larger is the distinguished ability. $\rho=0.4$ is usually used.

The r_i is the average value of the grey relational coefficients, which can be calculated by

$$r_i = \frac{1}{5}\sum_{k=1}^{5} \xi_i(k). \tag{5}$$

3 Results and discussion

3.1 Characterization of ESP/EFF ash

The SEM results of fly ash in units #1 and #14 are presented in Fig. 1. Because of the similar boiler types of units #1–#12 and #13–#15, only the results of units #1 and #14 are presented. The morphology of fly ash from PC boilers burning coal (unit #1) was distinguished from that from CFB boilers burning coal containing waste sludge (unit #14). The CFB boiler with small capacity of units #14 and #15 had a low burning temperature (850–900 °C) compared with the PC boiler (units #1–#12). The fly ash from PC boilers is mainly spherical whereas the fly ash from CFB boilers was irregular in shape, and had more pore structure. The results of particle size measurement are listed in Table 3. The relatively high particle size of fly

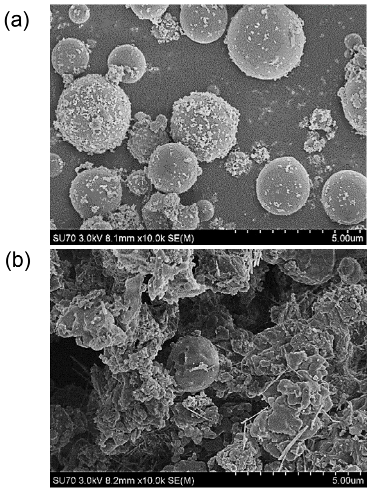

Fig. 1 Photo-micrographs of fly ash
(a) Unit #1; (b) Unit #14

ash in units #9 and #10 are probably due to different combustion characteristics and coal properties.

The concentrations of trace elements and contents of major oxides in fly ash and bottom ash are presented in Table 4. Most Hg, As, and Se would vaporize during combustion due to their high volatility (Bhangare et al., 2011), and subsequently condense on the surface of fly ash particles with the decreasing temperature of the flue gas. In this study, the concentrations of Hg, As, and Se in fly ash were at

Table 3 Median particle size of fly ash from tested units (unit: μm)

Unit	Median particle size	Unit	Median particle size	Unit	Median particle size
#1	11.4	#6	22.1	#11	41.2
#2	8.3	#7	27.6	#12	40.9
#3	23.6	#8	38.1	#13	42.1
#4	15.2	#9	58.1	#14	29.0
#5	19.0	#10	53.1	#15	35.0

Table 4 Concentrations of trace elements and contents of major oxides in fly ash and bottom ash

Unit	Trace metal (mg/kg)			Oxide (%)				
	Hg	As	Se	SiO_2	Al_2O_3	CaO	Fe_2O_3	SO_x
Fly ash								
#1	0.52	39.7	9.6	45.12	19.08	15.98	9.69	1.19
#2	0.16	26.6	7.6	48.44	25.40	11.55	5.40	1.33
#3	0.54	39.8	13.8	48.99	18.27	1.96	5.30	0.93
#4	0.29	22.9	12.6	46.56	36.92	6.05	3.50	0.83
#5	0.15	20.6	20.3	47.43	20.30	13.02	9.84	0.78
#6	0.28	39.6	24.9	46.26	41.67	4.02	2.74	0.54
#7	0.37	21.9	13.3	47.35	39.35	3.94	3.00	0.65
#8	0.24	30.3	10.6	49.10	28.57	3.55	9.37	0.69
#9	0.19	1.7	1.9	57.94	30.27	2.84	3.00	0.77
#10	0.06	3.4	2.1	47.40	32.04	8.76	6.61	0.64
#11	0.05	9.7	4.0	52.58	31.80	4.09	2.87	0.73
#12	0.06	18.6	4.3	54.48	28.68	4.61	4.33	1.24
#13	0.28	22.4	14.0	41.64	30.28	12.09	5.18	5.18
#14	0.38	28.5	19.5	34.70	25.82	16.60	11.18	2.68
#15	0.31	44.2	13.3	28.56	18.33	17.69	21.65	3.52
Bottom ash								
#1	0.0081	6.13	3.36	51.81	26.24	8.77	5.46	2.12
#2	0.0063	18.50	3.69	49.49	24.02	11.71	5.46	1.57
#3	0.0024	8.35	10.80	60.03	22.55	7.53	5.46	0.69
#4	0.0030	4.01	3.00	50.27	34.60	6.33	4.32	0.06
#5	0.0000	8.34	<0.01	50.38	31.49	7.25	5.22	1.00
#6	0.0116	6.66	0.63	46.80	40.73	4.99	3.00	0.56
#7	0.0001	5.02	<0.01	48.75	38.91	4.25	3.58	0.38
#8	<0.0001	15.60	8.45	49.69	30.87	2.69	9.18	2.63
#9	<0.0001	0.39	0.60	54.70	29.15	4.12	5.40	0.60
#10	<0.0001	1.72	0.34	37.58	23.94	8.43	8.31	1.04
#11	<0.0001	3.03	3.84	49.77	32.99	5.60	6.79	1.02
#12	<0.0001	6.83	0.27	48.55	25.09	10.21	7.03	2.31
#13	0.0051	13.50	0.46	44.70	31.64	8.41	2.75	7.89
#14	0.0007	20.90	2.32	24.86	15.87	30.67	16.14	3.03
#15	<0.0001	39.80	0.086	23.98	15.22	22.80	25.99	0.75

0.05 to 0.54 mg/kg, 1.7 to 44.2 mg/kg, and 1.9 to 24.9 mg/kg, respectively, which were generally higher than those in coal. The concentrations of Hg in the bottom ash were extremely low (<0.01 mg/kg). For As and Se, the concentrations ranged from 0.39 mg/kg to 39.8 mg/kg and <0.01 mg/kg to 10.8 mg/kg, respectively.

Fig. 2 shows the partition ratio of Hg, As, and Se between fly ash and bottom ash. The partition ratio is the ratio of concentration of an element in fly ash to its concentration in the bottom ash. For Hg, As, and Se, the partition ratios all exceeded unity, indicating that all elements were more enriched in the fly ash than in the bottom ash. Hg had the highest values of partition ratio (23.7–3740) for all tested coal fired power units due to its higher volatility compared to As (1.1–6.5) and Se (1.1–2027). The results were consistent with previous studies (Meij et al., 2002) in that the volatility order was Hg>Se>As.

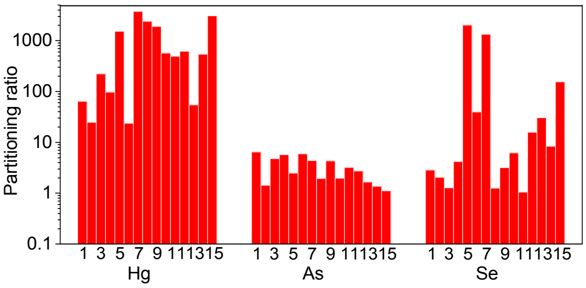

Fig. 2 Partition ratio of Hg, As, and Se between fly ash and bottom ash

3.2 Abatement capacity of Hg, As, and Se in dust removal devices

The mass distributions of Hg, As, and Se in the bottom ash, fly ash, and out of ESP, namely, $\mathrm{MD_{BA}}$, $\mathrm{MD_{FA}}$, and $\mathrm{MD_{ESP\text{-}OUT}}$, were analyzed to evaluate the abatement capacity for Hg, As, and Se in dust removal devices. The mass flows of coal, fly ash, and bottom ash, namely, m_{coal}, m_{FA}, and m_{BA}, were determined by the actual operational values during the sampling process. The mass distribution calculations are given by

$$\mathrm{MD_{FA}}=\frac{C_{i,\mathrm{FA}}\times m_{\mathrm{FA}}}{C_{i,\mathrm{coal}}\times m_{\mathrm{coal}}}\times 100\%, \tag{6}$$

$$\mathrm{MD_{BA}}=\frac{C_{i,\mathrm{BA}}\times m_{\mathrm{BA}}}{C_{i,\mathrm{coal}}\times m_{\mathrm{coal}}}\times 100\%, \tag{7}$$

$$\mathrm{MD_{ESP\text{-}OUT}}=(1-\mathrm{MD_{FA}}-\mathrm{MD_{BA}})\times 100\%, \tag{8}$$

where $C_{i,\mathrm{coal}}$, $C_{i,\mathrm{FA}}$, and $C_{i,\mathrm{BA}}$ represent the mean concentrations of trace elements in coal, fly ash, and bottom ash, respectively.

The results are presented in Fig. 3. Only 8.7%–36.1% of Hg escaped from LLT-ESP, whereas 42.1%–90.6% of Hg escaped from CS-ESP. The results indicate that LLT-ESP had greater abatement capacity for Hg than normal CS-ESP. The SCR system installed in the tested units might increase the transformation from $\mathrm{Hg^0}$ to $\mathrm{Hg^{2+}}$ (Pudasainee et al., 2010). The lower inlet temperature of LLT-ESP (<95 °C) resulted in a higher chance for the adsorption of volatile elements on the fly ash. Meanwhile, dust resistivity was greatly reduced in LLT-ESP, and this could improve collecting efficiency for PM as well as $\mathrm{Hg^p}$ (Zhang et al., 2016). The removal efficiency for Hg was extremely low for units #9–#12. That is probably due to the higher inlet temperature of CS-ESP (>125 °C) and the relatively large fly ash particle size (>40 μm). For units #9 and #10, the fly ash particle size was larger, so the physical adsorption capacity for volatile elements was limited. The feed coal of unit #12 had the lowest Cl content (67 mg/kg) and the highest S content (3.5%), which might inhibit $\mathrm{Hg^0}$ oxidation. The distribution of Hg in EFF of units #13, #14, and #15 reached 94%, 84%, and 99%, respectively. The cake layers formed in EFF could greatly enhance the catalytic oxidation and adsorption of Hg (Font et al., 2012).

Most of As was enriched in fly ash and bottom ash. The abatement capacity for As in dust removal devices was generally high, with only 0.9%–27.7% escaping from ESP and EFF. 70.7%–100% of Se was enriched in fly ash and bottom ash in units #1–#8. Only 1.9%–10.1% of Se escaped from EFF of units #13–#15. However, the fly ash and bottom ash of units #9–#12 only retained 34.2%–49.8% of total Se. The abatement capacity of CS-ESP in units #9–#12 was limited probably due to similar reasons as for Hg. It can be concluded that ESP with an inlet temperature <125 °C and EFF had a great abatement capacity for As and Se when the fly ash particle size is less than 40 μm.

3.3 Effects on the enrichment of Hg, As, and Se in fly ash

From the results above, LLT-ESP, CS-ESP, and EFF showed different abatement capacities for Hg, As, and Se, where the inlet temperature of ESP and particle size of fly ash might exert a huge impact. As well as these two factors, there were many other factors influencing the enrichment of Hg, As, and Se in fly ash. The content of iron oxides (Fe_2O_3) and calcium oxides (CaO) in fly ash, the contents of Cl, S as well as the value of Cl/S in feed fuel were important factors to the enrichment of volatile elements in fly ash. In addition, SO_3 might condense on the fly ash in LLT-ESP, and this could influence the adsorption of volatile elements. The effects of the aforementioned eight factors on the enrichment of trace elements in fly ash captured by ESP was analyzed by Pearson correlation analysis and grey relational analysis as follows.

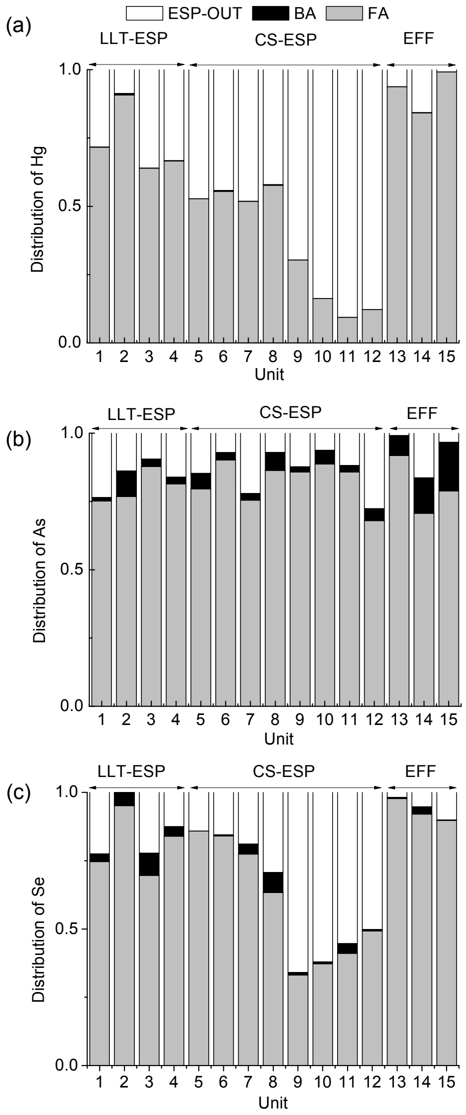

Fig. 3 Mass distribution of trace elements in bottom ash, fly ash, and ESP-OUT: (a) distribution of Hg; (b) distribution of As; (c) distribution of Se

3.3.1 Pearson correlation analysis

The relative enrichment factor (REF) is considered the most appropriate way to evaluate enrichment characteristics of trace elements in bottom ash and fly ash and has been widely used in previous studies (Meij et al., 2002; Bhattacharyya et al., 2009). The relative enrichment factor was calculated by

$$\mathrm{REF} = C_{i,\mathrm{ash}} \times C_{\mathrm{ash\text{-}in\text{-}coal}} \big/ C_{i,\mathrm{coal}}, \tag{9}$$

where $C_{\mathrm{ash\text{-}in\text{-}coal}}$ presents the ash content in coal.

The REF values were calculated to quantitatively analyze the enrichment of trace elements and the results are presented in Table S1 in the electronic supplementary materials. Relation charts of REF values of Hg, As, and Se in fly ash as a function of the eight factors are plotted in Fig. 4 to investigate the correlations between enrichment of Hg, As, and Se and influencing factors. EFF has a different dust removal mechanism from LLT-ESP and CS-ESP. Thus, the data of EFF were not included in the plots.

The results demonstrated that the enrichment of Hg, As, and Se in fly ash had negative correlations between ESP temperature, particle size, and S contents in the feed fuel and had positive correlations between Cl, Cl/S in feed fuel, Fe_2O_3, and REF values of S in fly ash. Pearson correlation coefficients handled by SPSS were analyzed in order to obtain the accurate results, which are presented in Fig. 4.

The absolute values of Pearson correlation coefficients ($|R|$) between the REF of Hg, As, and Se and influencing factors are divided into five categories according to the degree of correlation, which are listed in Table 5.

The inlet temperature and particle size of fly ash showed highly strong positive correlations with the REF of Hg in fly ash. The results validate that low temperature in LLT-ESP gives an enormous promotion for the enrichment of Hg in fly ash and Hg tends to be absorbed on the surface of finer particles (Jew et al., 2015). The higher REF value of S was mainly caused by the condensation of SO_3 on fly ash. The strong positive correlations between Hg and the REF-S indicated that Hg in the flue gas could be captured simultaneously with SO_3 in the LLT-ESP.

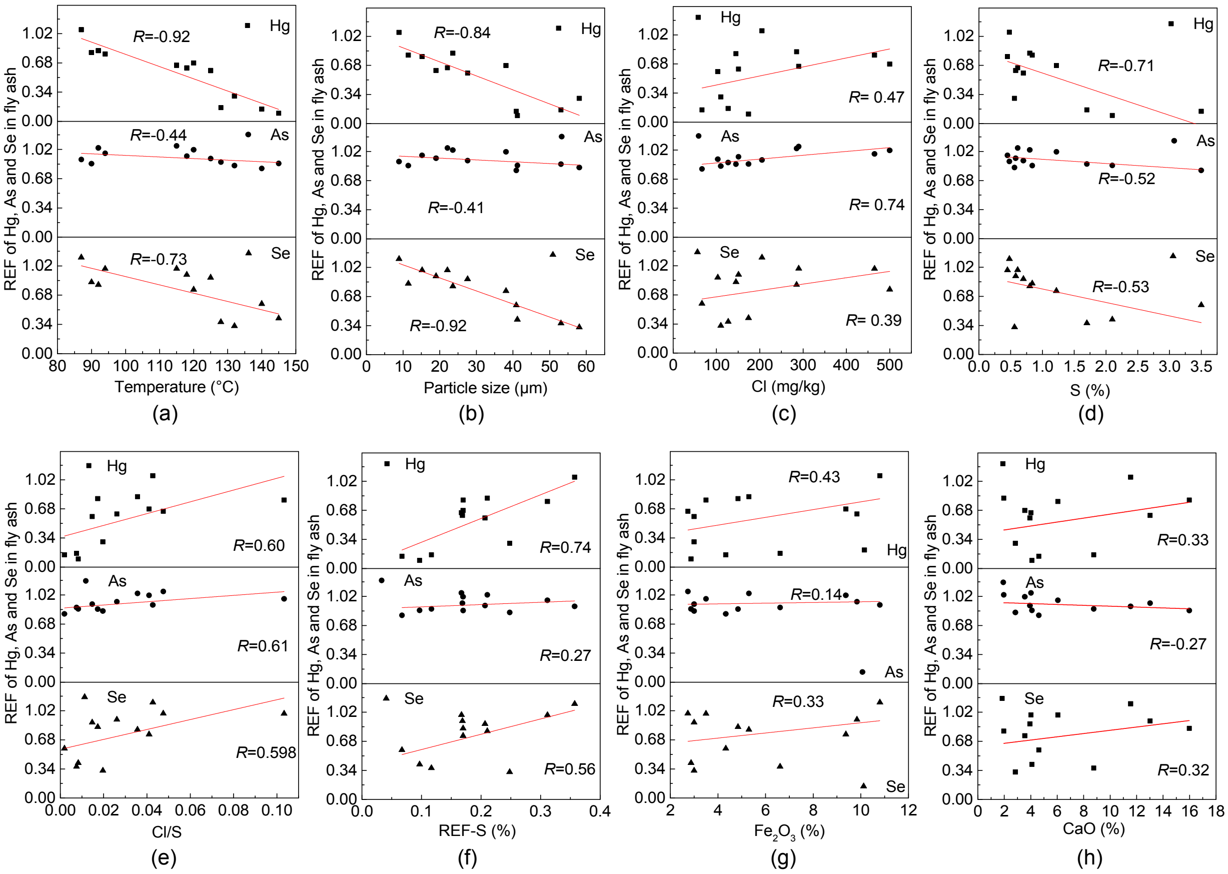

Fig. 4 Correlations between REF values of Hg, As, and Se in fly ash and influencing factors

(a) Temperature; (b) Particle size; (c) Cl; (d) S; (e) Cl/S; (f) REF-S; (g) Fe_2O_3; (h) CaO

Table 5 Results of Pearson correlation analysis

|*R*|	Degree of correlation	Trace element		
		Hg	As	Se
0.8–1.0	Highly strong	*T*>particle size	–	Particle size>*T*
0.6–0.8	Strong	REF-S>S	Cl>Cl/S	–
0.4–0.6	Moderate	Cl/S>Cl>Fe_2O_3	S	REF-S>Cl/S>S
0.2–0.4	Weak	CaO	*T*>particle size	Cl>Fe_2O_3>CaO
0.0–0.2	Very weak	–	REF-S>CaO>Fe_2O_3	–

T: temperature

The competition of SO_3 for the adsorption sites was limited in LLT-ESP and the condensation of SO_3 might offer active adsorption sites for Hg to form $HgSO_4$ on the fly ash according to

$$2SO_3+2Hg+O_2 \rightarrow 2HgSO_4. \tag{10}$$

The content of S in feed fuel showed a strong negative correlation with the REF of Hg in fly ash. The inhibitory effect of SO_2 on the oxidation of mercury may be due to the reaction between SO_2 and Cl_2 (López-Antón et al., 2009) or the competition of oxidation by SO_2 (Liu et al., 2012) as follows:

$$SO_2(g)+Cl_2(g) \rightarrow SO_2Cl_2(g), \tag{11}$$

$$HgO\,(s)+SO_2(g) \rightarrow Hg^0(g)+SO_3(g). \tag{12}$$

The contents of Cl and Cl/S in coal had moderately positive correlations. Higher contents of Cl in feed fuel promoted the presence of HCl and the subsequent formation of gaseous $HgCl_2$ (Wang et al., 2010; Zhang et al., 2016), which lead to the chemical adsorption of Hg on the fly ash (Presto and Granite, 2007; López-Antón et al., 2009; Ochiai et al., 2009). The content of Fe_2O_3 also had a moderately positive correlation with Hg in fly ash whereas the contents of CaO had a weak correlation. That is probably because iron oxides (Fe_2O_3) contained in fly ash had strong catalytic oxidation activity for Hg^0 in the flue gas (Ghorishi et al., 2005; Jung et al., 2015).

For As, the chorine in coal had strong positive correlations whereas S had a moderately negative correlation. Chlorides might be conducive to the reaction of arsenic oxides with the minerals in the fly ash via forming As-Cl bond species (Urban and Wilcox, 2006) while SO_2 hindered the adsorption.

The inlet temperature of ESP and the particle size had weak correlations. The content of CaO, Fe_2O_3, and REF-S in fly ash showed a very weak correlation. The enrichment of As in fly ash was partly affected by the amount of As retained in bottom ash and the variations between REF values of As are small. Therefore, the correlations of most factors were relatively weak and the results might be affected by random error.

The particle size of fly ash had the highest Pearson correlation coefficient for Se, which indicated that physical adsorption was the dominating adsorptive mode for Se. The inlet temperature of ESP also had a highly strong effect on the adsorption of Se in fly ash. The correlation of REF-S with REF of Se was probably due to the synchronization effects of temperature on SO_3 and Se. Similar to Hg and As, the S content in coal had a negative correlation with the REF of Se.

3.3.2 Grey relational analysis

The relation charts with Pearson correlation analysis provide the intuitive linear correlations between REF values and individual influencing factors. However, the correlations between the factors and enrichment of trace metals in fly ash are not necessarily linear. The influencing mechanisms of the factors are mutual and complex. Therefore, it is necessary to quantitatively analyze the factors at the same time and discover the significance level of each factor. Grey relational analysis was employed to determine the significance level of eight factors on the REF of fly ash for Hg, As, and Se.

The results of the grey relational grades are presented in Fig. 5, and the detailed data processing is provided in Tables S2–S4 in electronic supplementary materials. The order of grey relational grades values for REF of Hg was: REF-S (0.766)>particle size (0.765)>S (0.76)>T (0.73)>Cl/S (0.72)>Cl (0.68)>Fe_2O_3 (0.66)>CaO (0.61). Among all the factors, the effects of REF-S, particle size of fly ash, the content of S, and temperature showed higher significance. This is consistent with the Pearson coefficients. However, the specific order of Pearson coefficients and grey relational grade was different. For As, the order was T (0.88)>REF-S (0.77)>S (0.73)>Cl (0.72)>Fe_2O_3 (0.71)>particle size (0.70)>Cl/S (0.68)>CaO (0.65). The order was different from the results of Pearson coefficients in that the grey relational grade of temperature was the highest, which indicated that when comparing the change of all the factors together, temperature was the key factor to the enrichment of As. In addition, the deviations of REF values of As were not very obvious among the tested units, which might explain why the grey relational grades were generally higher whereas the linear correlations were not very strong. With respect to Se, the order was S (0.83)>T (0.82)>REF-S (0.76)>particle size (0.72)> Fe_2O_3 (0.69)>Cl (0.67)>Cl/S (0.65)>CaO (0.62). The S content in coal and temperature of ESP were the dominant factors. The results indicate that SO_2 in the flue gas might hinder the adsorption of Se.

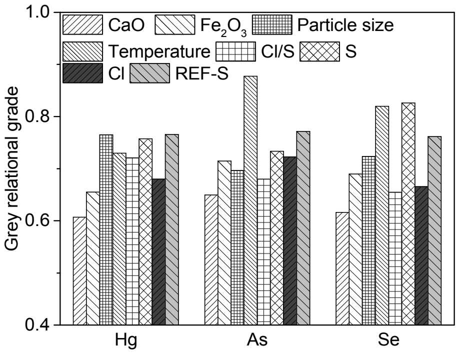

Fig. 5 Grey relational analysis for REF values of Hg, As, and Se with influencing factors

The grey relational analysis offered a more comprehensive analysis than Pearson correlations. However, when the deviations of REF values were not obvious, the results of grey relational grades might not be precise. Based on the results of the

Pearson correlation analysis and grey relational analysis, it can be concluded that inlet temperature of the ESP had a significant effect on the enrichment of higher volatile elements. Therefore, LLT-ESP has the advantage of capturing Hg, As, and Se. The particle size of fly ash also had a great effect on the adsorption of Hg and Se. Smaller particle size was conducive to the physical adsorption for highly volatile elements. The inhibitory effect of sulfur content was obvious for Hg and Se. Higher content of chlorine and lower content of sulfur can be more conducive to the accumulation of Hg, As, and Se in fly ash. The simultaneous removal of SO_3 and trace elements could be achieved in LLT-ESP. In this case, the transformation of chloride forms of trace elements to sulfate forms could be promoted, and this was beneficial for the disposal of fly ash as the sulfur forms of heavy metals have less toxicity. The iron oxides in fly ash had positive correlations with Hg and Se. However, the effects were limited compared with other factors.

4 Conclusions

LLT-ESP and EFF had great abatement capacity for Hg compared with normal CS-ESP. Only 0.8%–36.1% of Hg escaped from LLT-ESP and EFF, whereas 42.1%–90.6% of Hg escaped from CS-ESP. With the employment of EFF and ESP (inlet temperature <125 °C), 72.3%–99.1% of As and 70.7%–100% of Se could be removed before the WFGD system. Coal-fired power plants equipped with LLT-ESP could not only effectively capture dust but also hazardous trace elements as the co-benefit to achieve ultra-low emissions of multi-pollutants.

Inlet temperature of ESP has a significant effect on the enrichment of higher volatile elements. The simultaneous removal of SO_3 and trace elements could be achieved in LLT-ESP. The particle size of fly ash also has a great influence on the adsorption of Hg, As, and Se. The inhibitory effect of sulfur content was significant for Hg and Se. Higher content of chlorine and lower content of sulfur in coal can be conducive to the accumulation of Hg, As, and Se in fly ash. The effects of content of oxides (CaO and Fe_2O_3) in the fly ash were limited compared with other factors. To sum up, the optical conditions for Hg, As and Se removal are lower inlet temperature of ESP, smaller particle size of fly ash, higher contents of chlorine and oxides (CaO and Fe_2O_3) with lower content of sulfur in coal.

References

Bhangare RC, Ajmal PY, Sahu SK, et al., 2011. Distribution of trace elements in coal and combustion residues from five thermal power plants in India. *International Journal of Coal Geology*, 86(4):349-356. https://doi.org/10.1016/j.coal.2011.03.008

Bhattacharyya S, Donahoe RJ, Dan P, 2009. Experimental study of chemical treatment of coal fly ash to reduce the mobility of priority trace elements. *Fuel*, 88(7):1173-1184. https://doi.org/10.1016/j.fuel.2007.11.006

Burmistrz P, Kogut K, Marczak M, et al., 2016. Lignites and subbituminous coals combustion in polish power plants as a source of anthropogenic mercury emission. *Fuel Processing Technology*, 152:250-258. https://doi.org/10.1016/j.fuproc.2016.06.011

Chen JC, Wey MY, Liu ZS, 2001. Adsorption mechanism of heavy metals on sorbents during incineration. *Journal of Environmental Engineering*, 127(1):63-69. https://doi.org/10.1061/(ASCE)0733-9372(2001)127:1(63)

Cheng CM, Hack P, Chu P, et al., 2009. Partitioning of mercury, arsenic, selenium, boron, and chloride in a full-scale coal combustion process equipped with selective catalytic reduction, electrostatic precipitation, and flue gas desulfurization systems. *Energy & Fuels*, 23(10):4805-4816. https://doi.org/10.1021/ef900293u

Deng S, Shi YJ, Liu Y, et al., 2014. Emission characteristics of Cd, Pb and Mn from coal combustion: field study at coal-fired power plants in China. *Fuel Processing Technology*, 126:469-475. https://doi.org/10.1016/j.fuproc.2014.06.009

Font O, Cordoba P, Leiva C, et al., 2012. Fate and abatement of mercury and other trace elements in a coal fluidised bed oxy combustion pilot plant. *Fuel*, 95(1):272-281. https://doi.org/10.1016/j.fuel.2011.12.017

Fu YY, Ma K, 2014. Application of low-low temperature ESP technology in thermal power plant. *Advanced Materials Research*, 1070-1072:1481-1485.

Futsaeter, G., Wilson, S, 2013. The UNEP global mercury assessment: sources, emissions and transport. E3S Web of Conferences, 1:36001. https://doi.org/10.1051/e3sconf/20130136001

Gao YS, Zhang Z, Wu JW, et al., 2013. A critical review on the heterogeneous catalytic oxidation of elemental mercury in flue gases. *Environmental Science & Technology*, 47(19):10813-10823. https://doi.org/10.1021/es402495h

GAQSIQ (General Administration of Quality Supervision, Inspection and Quarantine of the People's Republic of China), 2007. Determination of Total Sulfur in Coal, GB/T 214-2007 (in Chinese).

GAQSIQ (General Administration of Quality Supervision, Inspection and Quarantine of the People's Republic of

China), 2008. Proximate Analysis of Coal, GB/T212-2008 (in Chinese).

GAQSIQ (General Administration of Quality Supervision, Inspection and Quarantine of the People's Republic of China), 2014. Determination of chlorine in coal, GB/T 3558-2014 (in Chinese).

Ghorishi SB, Lee CW, Jozewicz WS, et al., 2005. Effects of fly ash transition metal content and flue gas HCl/SO_2 ratio on mercury speciation in waste combustion. *Environmental Engineering Science*, 22(2):221-231. https://doi.org/10.1089/ees.2005.22.221

Hower JC, Senior CL, Suuberg EM, et al., 2010. Mercury capture by native fly ash carbons in coal-fired power plants. *Progress in Energy and Combustion Science*, 36(4):510-529. https://doi.org/10.1016/j.pecs.2009.12.003

Jew AD, Rupp EC, Geatches DL, et al., 2015. Mercury interaction with the fine fraction of coal-combustion fly ash in a simulated coal power plant flue gas stream. *Energy & Fuels*, 29(9):6025-6038. https://doi.org/10.1021/acs.energyfuels.5b01253

Jung JE, Geatches DL, Lee K, et al., 2015. First-principles investigation of mercury adsorption on the α-Fe_2O_3(1-102) surface. *Journal of Physical Chemistry C*, 119(47): 26512-26518. https://doi.org/10.1021/acs.jpcc.5b07827

Kellie S, Cao Y, Duan YF, et al., 2005. Factors affecting mercury speciation in a 100-MW coal-fired boiler with low-NO_x burners. *Energy & Fuels*, 19(3):800-806. https://doi.org/10.1021/ef049769d

Kuo Y, Yang T, Huang GW, 2008. The use of grey relational analysis in solving multiple attribute decision-making problems. *Computers & Industrial Engineering*, 55(1): 80-93. https://doi.org/10.1016/j.cie.2007.12.002

Liu J, Qu W, Sang WJ, et al., 2012. Effect of SO_2 on mercury binding on carbonaceous surfaces. *Chemical Engineering Journal*, 184(2):163-167. https://doi.org/10.1016/j.cej.2012.01.023

Lopez-Anton MA, Abad-Valle P, Diaz-Somoano M, et al., 2009. The influence of carbon particle type in fly ashes on mercury adsorption. *Fuel*, 88(7):1194-1200. https://doi.org/10.1016/j.fuel.2007.07.029

López-Antón MA, Diaz-Somoano M, Spears DA, et al., 2006. Arsenic and selenium capture by fly ashes at low temperature. *Environmental Science & Technology*, 40(12): 3947-3951. https://doi.org/10.1021/es0522027

Meij R, Vredenbregt LHJ, Winkel HT, 2002. The fate and behavior of mercury in coal-fired power plants. *Journal of the Air & Waste Management Association*, 52(8): 912-917. https://doi.org/10.1080/10473289.2002.10470833

MEP (Ministry of Environmental Protection of the People's Republic of China), 2011. Emission Standard of Air Pollutants for Thermal Power Plants, GB 13223-2011 (in Chinese).

Ochiai R, Uddin MA, Sasaoka E, et al., 2009. Effects of HCl and SO_2 concentration on mercury removal by activated carbon sorbents in coal-derived flue gas. *Energy & Fuels*, 23(10):4734-4739. https://doi.org/10.1021/ef900057e

Presto AA, Granite EJ, 2007. Impact of sulfur oxides on mercury capture by activated carbon. *Environmental Science & Technology*, 41(18):6579-6584. https://doi.org/10.1021/es0708316

Pudasainee D, Lee SJ, Lee SH, et al., 2010. Effect of selective catalytic reactor on oxidation and enhanced removal of mercury in coal-fired power plants. *Fuel*, 89(4):804-809. https://doi.org/10.1016/j.fuel.2009.06.022

Tian HZ, Wang Y, Xue ZG, et al., 2010. Trend and characteristics of atmospheric emissions of Hg, As, and Se from coal combustion in China, 1980-2007. *Atmospheric Chemistry and Physics*, 10(23):11905-11919. https://doi.org/10.5194/acp-10-11905-2010

Tian HZ, Liu KY, Zhou JR, et al., 2014. Atmospheric emission inventory of hazardous trace elements from China's coal-fired power plants--temporal trends and spatial variation characteristics. *Environmental Science & Technology*, 48(6):3575-3582. https://doi.org/10.1021/es404730j

Urban DR, Wilcox J, 2006. A theoretical study of properties and reactions involving arsenic and selenium compounds present in coal combustion flue gases. *Journal of Physical Chemistry A*, 110(17):5847-5852. https://doi.org/10.1021/jp055564+

Wang SX, Zhang L, Li GH, et al., 2010. Mercury emission and speciation of coal-fired power plants in China. *Atmospheric Chemistry and Physics*, 10(3):1183-1192. https://doi.org/10.5194/acp-10-1183-2010

Wilcox J, Rupp E, Ying SC, et al., 2012. Mercury adsorption and oxidation in coal combustion and gasification processes. *International Journal of Coal Geology*, 90:4-20. https://doi.org/10.1016/j.coal.2011.12.003

Zhang L, Wang SX, Wu QR, et al., 2016. Mercury transformation and speciation in flue gases from anthropogenic emission sources: a critical review. *Atmospheric Chemistry and Physics*, 16(4):2417-2433. https://doi.org/10.5194/acp-16-2417-2016

Zhou ZJ, Liu XW, Zhao B, et al., 2015. Effects of existing energy saving and air pollution control devices on mercury removal in coal-fired power plants. *Fuel Processing Technology*, 131:99-108. https://doi.org/10.1016/j.fuproc.2014.11.014

List of electronic supplementary materials

Table S1 Relative enrichment factors

Table S2 Data processing of grey relational grade of factors on REF of Hg

Table S3 Data processing of grey relational grade for REF of As

Table S4 Data processing of grey relational grade of factors on REF of Se

中文概要

题　目：超低排放电厂除尘器对痕量重金属的控制作用

目　的：燃煤过程中释放的痕量重金属迁移到大气中会对人体造成很大的危害。除尘器在脱除颗粒物的同时可以协同脱除重金属，研究超低排放除尘器对重金属的控制作用效果和影响因素，可以得到提升脱除重金属效率的手段和方法，利于实现燃煤电厂重金属的超低排放。

方　法：1. 通过测试方法检测出重金属在煤、飞灰和底灰当中的绝对含量；2. 通过分析重金属在飞灰和底灰中占总输入量的比例，得到三种类型除尘器对重金属的脱除效果；3. 通过皮尔森相关性系数和灰色关联模型分析各影响因素对重金属在飞灰当中富集的影响作用大小。

结　论：1. 低温电除尘器和电袋除尘器对于汞、砷和硒的脱除效果明显大于常规电除尘器；2. 电除尘器的入口烟气温度越低，汞、砷和硒在除尘器中的脱除效果越好；3. 煤中的硫含量对重金属在飞灰当中的吸附作用影响明显，其含量越高越不利于重金属的吸附；4. 与其他影响因素相比，飞灰当中的铁氧化物和钙氧化物对重金属在飞灰当中吸附的促进作用较为有限。

关键词：超低排放；除尘器；重金属；影响因素